

Zero-Magnetic-Field Hall Effect in Broken-Mirror-Symmetry Conductors under Illumination

Victor M. Edelstein

Institute for Solid State Physics of RAS, Chernogolovka, 142432 Moscow District, Russia

(Received 31 January 2005; published 5 October 2005)

A novel effect is predicted for conductors with a broken mirror symmetry [e.g., polar metals and asymmetrical quantum well (QW) structures]: if such a conductor is under the direct current $\mathbf{J} \sim \mathbf{E}^{(d)}$, the circular polarized infrared radiation should induce an additional transverse current $\mathbf{J}_H \sim \mathbf{E}^{(d)} \times \mathbf{c}$, where $\mathbf{E}^{(d)}$ is the driving electric field and \mathbf{c} is a vector directed either along the polar axis or perpendicular to a QW. The sign of the current \mathbf{J}_H can be reversed by switching the helicity of the light from right to left-handed. Thus the phenomenon is, in fact, something like the Hall effect in which light acts as an external magnetic field.

DOI: 10.1103/PhysRevLett.95.156602

PACS numbers: 72.40.+w, 71.70.Ej, 42.65.-k, 78.66.-w

It is believed that the invariance under space reflections imposes heavy constraints on the possible behavior of physical systems. The majority of conducting crystals have a center of symmetry. However, there are also quite a number of bulk three-dimensional (3D) and quasi-two-dimensional (2D) semiconductors and metals with a broken mirror symmetry. These are compounds whose symmetry group includes a polar axis [e.g., Mo_3AlC (symmetry $P4_132$) and Mo_3P (symmetry $I\bar{4}$) [1]], some narrow-gap semiconductor heterostructures with violated “up-down” symmetry (e.g., $\text{In}_x\text{Ga}_{1-x}\text{As}/\text{In}_y\text{Al}_{1-y}\text{As}$ [2]), and 2D bands at the surfaces of some metals (Au [3], W, and Mo [4]). Although there are no parity constraints in these conductors, it is not at all obvious whether this fact can have an effect on their electric properties. In this Letter we try to draw attention to a new feature in electrodynamics which distinguishes the mirror-odd conductors from usual, center-symmetric ones.

The topic is also relevant to spintronics [5], because just the coupling between spin and orbital degrees of freedom is the main factor through which the mirror symmetry violation reveals itself in dynamics of electrons in such compounds. In fact, the violation of mirror symmetry gives rise to the additional term

$$H_{\text{so}} = \frac{\alpha}{\hbar} (\mathbf{p} \times \mathbf{c}) \cdot \vec{\sigma} \quad (1)$$

in the Hamiltonian of the carriers [6], where \mathbf{p} , $\vec{\sigma}$, and \mathbf{c} are, respectively, the electron momentum, the Pauli matrices, and the unit vector directed either along the polar axis or perpendicular to the asymmetric 2D structure. This spin-orbit (SO) coupling has recently become the focus of many theoretical and experimental studies [7]. The present Letter sheds light on a quite new aspect of the coupling: a possibility of controlling the electric current with the aid of light.

The possibility of the effect can be understood in a rather intuitive way. The term (1) can be viewed as the Zeeman energy in a fictitious magnetic field $\mathbf{B}_f = \alpha(\mathbf{p} \times \mathbf{c})/\mu_B g$ which influences the electron kinetic in two ways. First, it

stochastically changes its direction by scattering on impurities resulting in a finite time of the spin relaxation $\tau_{\text{so}} \approx \tau(\alpha p_F \tau / \hbar^2)^{-2}$, where p_F is the Fermi momentum and τ is the elastic lifetime due to impurities [8]. Second, if under the action of an electric field \mathbf{E} , the electric current $\mathbf{J} \sim \mathbf{E}$ passes through the system (so that the ensemble-averaged momentum $\langle \mathbf{p} \rangle \sim \mathbf{J}$), the average field $\langle \mathbf{B}_f \rangle$ induces a spin polarization of the carriers proportional to $\mathbf{c} \times \mathbf{E}$ [9]. This magnetoelectric effect (MEE) means that under the action of the electric field \mathbf{E} a correction to the electron distribution function arises which is proportional to $\vec{\sigma} \cdot (\mathbf{c} \times \mathbf{E})$. In the case when the field is the radiation field (that can be presented as $\mathbf{E}_\omega^{(l)} e^{i\omega t} + \mathbf{E}_\omega^{(l)*} e^{-i\omega t}$) one can assume that in the second order perturbation theory, the field may induce a correction to the distribution function of the form $[\vec{\sigma} \cdot (\mathbf{c} \times \mathbf{E}_\omega^{(l)})][\vec{\sigma} \cdot (\mathbf{c} \times \mathbf{E}_\omega^{(l)*})]$, which is simply $i(\vec{\sigma} \cdot \mathbf{c})(\mathbf{c} \cdot \mathbf{E}_\omega^{(l)} \times \mathbf{E}_\omega^{(l)*})$. This correction means that the illumination of the system by circular polarized light induces a permanent spin magnetization $\mathbf{M} \sim i\mathbf{c}(\mathbf{c} \cdot \vec{\epsilon} \times \vec{\epsilon}^*)$, where $\vec{\epsilon}$ is the polarization vector. In other words, this is the inverse Faraday effect (IFE) [10]. Thus the effect of circular polarized light on *electron spins* of the mirror-odd conductor is very much like the effect of an external magnetic field. By pursuing the analogy further, a question arises: is the effect of the light on *the electric current* the same as the effect of an external magnetic field. Indeed, since an external magnetic field applied to a system with SO coupling can induce the Hall effect not only via the Lorentz force, but also through the Zeeman interaction with the electron spins [11], one could anticipate that if a mirror-odd crystal is under the direct current $\mathbf{J} \sim \mathbf{E}^{(d)}$, the circular polarized light illumination will induce the pseudo-Hall effect; i.e., the occurrence of the transverse current $\mathbf{J}_H \sim \mathbf{M} \times \mathbf{E}^{(d)}$ *in the absence of any external magnetic field*.

Here it will be shown that in the case of a 2D electron system and high enough light frequencies $\omega\tau > 1$ the total current takes the form

$$\mathbf{J} = \sigma_D \mathbf{E}^{(d)} + \sigma_H (\mathbf{c} \times \mathbf{E}^{(d)}) i(\mathbf{c} \cdot \vec{\epsilon} \times \vec{\epsilon}^*), \quad (2)$$

where $\sigma_D = (e^2/\pi)\epsilon_F\tau$ is the 2D Drude conductivity, $\vec{\epsilon}$ is the polarization vector of the light, $\epsilon_F = p_F^2/m$ is the Fermi energy

$$\sigma_H = \sigma_D \left(\frac{eE_\omega^{(l)}\tau}{p_F} \right)^2 \frac{2\eta\delta}{(\omega\tau)(\epsilon_F\tau)} \left[2\eta^2 - \frac{3}{2(\omega\tau)^4} \right], \quad (3)$$

$E_\omega^{(l)}$ is the value of the electric field of the light $\eta = 2\alpha p_F\tau$, $\delta = \alpha m/p_F$, and units are used in which $\hbar = c = 1$. (Corrections to the diagonal part of the conductivity tensor due to the illumination may be omitted.) Note that the pseudo-Hall current is quite different from a direct photocurrent induced by circular polarized radiation [12]. The former does not suppose any interband electron transitions and has a maximum at the normal light incidence, whereas the latter involves virtual (or real) dipole-allowed transitions between the conduction and valence bands and vanishes under such conditions.

So let us consider a 2D system (3D systems may be treated in the same way) with the Hamiltonian

$$H_0 = \frac{\hat{\mathbf{p}}^2}{2m} + \alpha(\hat{\mathbf{p}} \times \mathbf{c}) \cdot \vec{\sigma} + \sum_i u\delta(\mathbf{r} - \mathbf{R}_i), \quad (4)$$

where $\hat{\mathbf{p}} = -i\nabla$, \mathbf{r} is the position of an electron and \mathbf{R}_i are the positions of the randomly distributed short-ranged impurities of concentration n_{imp} . The Hamiltonian of the system at the presence of the external fields, which are the driving electric field specified by the vector potential $\mathbf{A}^{(d)}$ and the field of the light specified by the vector potential $\mathbf{A}^{(l)}$, is obtained from H_0 by the substitution $\hat{\mathbf{p}} \rightarrow \hat{\mathbf{p}} + e\mathbf{A}$, $\mathbf{A} = \mathbf{A}^{(d)} + \mathbf{A}^{(l)}$ and can be represented as $H_0 + H_{\text{int}}$. We retain in H_{int} only the term $e\mathbf{v} \cdot \mathbf{A}$, where $\mathbf{v} = i[H_0(\mathbf{p}), \mathbf{r}] = \frac{\mathbf{p}}{m} + \alpha(\mathbf{c} \times \vec{\sigma})$ is the velocity operator, because the term of the second order in \mathbf{A} does not contribute to the pseudo-Hall current. As seen from (2) and (3), this current occurs as the third-order response to $e\mathbf{v} \cdot \mathbf{A}$: it is linear in $\mathbf{A}^{(d)}$ and quadratic in $\mathbf{A}^{(l)}$. Just as in [13], we consider $\mathbf{A}^{(d)}$ to have a small but finite frequency ω_0 . Since the final result depends only upon the combination $i\omega_0\mathbf{A}_{\omega_0}^{(d)} = \mathbf{E}_{\omega_0}^{(d)}$, the constant-driving field limit is obtained by letting $\omega_0 \rightarrow 0$ at the end of the calculations.

To calculate the response, we use the method introduced in [14] according to which, to study dynamical properties of a many-body system, the general procedure is to calculate first certain imaginary-time-ordered thermal correlation function, and then to perform an analytic continuation from the positive imaginary frequency axis to the real frequency axis, with respect to every external frequency, in order to obtain the corresponding physical, causal correlation function. So at the starting point, the external fields are considered as functions of discrete boson frequencies $\omega_n = i\pi 2nT$. The current density in the uniform system is given by the expression

$$\mathbf{J}(\omega_n) = T \sum_{\epsilon_l} \int \frac{d^2p}{(2\pi)^2} \text{Tr}\{-e\mathbf{v}G(\epsilon_l, \epsilon_l - \omega_n; \mathbf{p})\}, \quad (5)$$

where $\epsilon_l = i\pi T(2l + 1)$ and the exact electron Green function $G(\epsilon_l, \epsilon_l - \omega_n; \mathbf{p})$ includes, in addition to the external electromagnetic fields, also the impurity self-energies. By expanding $G(\epsilon_l, \epsilon_l - \omega_n; \mathbf{p})$ in powers of the external fields and omitting temporarily the effects of impurities, one gets $T^3 \sum_{\omega_{n_1}, \omega_{n_2}, \omega_{n_3}} T^{-1} \delta_{\omega_{n_1} + \omega_{n_2} + \omega_{n_3}, \omega_n} G(\epsilon_l)H_{\text{int}}(\omega_{n_1}) G(\epsilon_l - \omega_{n_1})H_{\text{int}}(\omega_{n_2}) G(\epsilon_l - \omega_{n_1} - \omega_{n_2}) \times H_{\text{int}}(\omega_{n_3}) G(\epsilon_l - \omega_{n_1} - \omega_{n_2} - \omega_{n_3})$, where one-frequency G functions are the free Green functions and all variables except for frequencies are suppressed for simplicity. So the expression for the current becomes three fermion loops. Each loop threads through four frequency bearing vertices which include one response velocity vertex and three cause vertices. One of the cause vertices represents the interaction with the driving field, $e\mathbf{v} \cdot \mathbf{A}^{(d)}$, and will be called the driving vertex. The other two cause vertices represent the interaction with the light, $e\mathbf{v} \cdot \mathbf{A}^{(l)}$, and will be called the light vertices. The loops are distinguished by relative positions of the driving and light vertices. Each term of the summation over ϵ_l in (5) can be regarded as the residue of an integral around the point $z = \epsilon_l$ so that one can transform $T \sum_{\epsilon_l} \rightarrow (4\pi i)^{-1} \oint_C dz \tanh(z/2T)$ followed by the deformation of the contour integral into the straight line integrals along $z = \epsilon \pm i0^+$, $z = \epsilon + \omega_{n_1} \pm i0^+$, \dots , where $\epsilon \in (-\infty, \infty)$ is the real integral variable. Referring the reader to [14] for details of the analytical continuation of these integrals, we give the final result. Every fermion loop becomes five diagrams: one retarded diagram that involved the product of only retarded Green functions $G^R(\epsilon) \times H_{\text{int}}(\omega_1)G^R(\epsilon - \omega_1) \dots$ multiplied by $\tanh(\frac{\epsilon - \omega_0}{2T})$, one advanced diagram that involved the product of only advanced Green function $G^A(\epsilon)H_{\text{int}}(\omega_1) \times G^A(\epsilon - \omega_1) \dots$ multiplied by $-\tanh(\frac{\epsilon}{2T})$, and three diagrams which will be called kinetic. The latter involve the products of retarded and advanced Green functions, so that the first Green function $G^R(\epsilon)$ is retarded, the last one $G^A(\epsilon - \omega_1 - \omega_2 - \omega_3)$ is advanced, and a change from a retarded to an advanced Green function occurs in any, but only one, cause vertex (the so-called ‘‘anomalous’’ vertex). The product has to be multiplied by the function (which can be considered as associated with this anomalous vertex) $F(\epsilon', \Omega) = [\tanh\frac{\epsilon'}{2T} - \tanh\frac{\epsilon' + \Omega}{2T}]$, where ϵ' and $\epsilon' + \Omega$ are the electron frequencies entering and leaving the vertex. All frequencies of the ‘‘continued’’ diagrams ($\omega_0, \omega_1, \dots$) are real, the discrete summation $T \sum_{\omega_{n_i}}$ is replaced by a continuous integral $(2\pi)^{-1} \int d\omega_i$, the Kronecker delta $T^{-1} \delta_{\omega_n, \omega_n'}$ by the Dirac delta $(2\pi)\delta(\omega - \omega')$, and the integration $(4\pi i)^{-1} \int_{-\infty}^{\infty} d\epsilon$ is finally performed. For the following analysis it is convenient to represent the current as $J_i = Q_{ij}(\omega_0)A_j^{(d)}(\omega_0)$ and discuss diagrams for $Q_{ij}(\omega_0)$.

The retarded and advanced diagrams do not contribute to the current. The kinetic diagrams with allowance for the effect of impurity scattering are shown in Fig. 1. The vertex with a wavy line represents $e\mathbf{v} \cdot \mathbf{A}_{\pm\omega}^{(l)}$ (two wavy lines have opposite frequencies). The free Green function (single line) has the form $G_{\alpha\beta}^{R(A)}(\zeta, \mathbf{p}) = \sum_{\nu=\pm} \Pi_{\alpha\beta}^{(\nu)}(\mathbf{p}) \times G_{\nu}^{R(A)}(\zeta, p)$, $G_{\nu}^{R(A)}(\zeta, p) = [\zeta - E_{\nu}(p) \pm \frac{i}{2\tau}]^{-1}$. Here $E_{\pm}(p) = \frac{p^2}{2m} \pm \alpha p$ are two branches of the energy spectrum of $H_0(\mathbf{p})$ of positive and negative helicities (the projection of a spin on the $\mathbf{p} \times \mathbf{c}$ direction) with the Fermi momenta $p_{\pm} \cong p_F(1 \mp \delta)$, $p_F = (2m\epsilon_F)^{1/2}$ and the densities of states at the Fermi level $N_{\pm} \cong (1 \mp \delta) \times \frac{m}{2\pi}$. $\Pi^{\pm}(\mathbf{p}) = \frac{1}{2}[1 \pm (\hat{\mathbf{p}} \times \mathbf{c}) \cdot \hat{\sigma}]$ are the corresponding projection operators. The SO constant α enters into a diagram through the parameters η and δ . The parameter η can be of the order of unity in real systems. Therefore, it is regarded as small only to simplify the calculations, so that all the necessary powers of η should be included. The parameter δ responsible for the difference between the branches is small $\delta/\eta = (4/\epsilon_F\tau) \ll 1$. Therefore, all powers of δ in excess of the first can be ignored. In other respects, the evaluation of diagrams can be performed by standard methods [13].

The diagrams of Fig. 1 fall into two groups. In the first diagrams shown in Fig. 1(a), the driving vertex is anomalous. In the second type of diagrams depicted in Figs. 1(b) and 1(c), one of the light vertices is anomalous. Note that the diagrams presented in Fig. 1 are similar to those for the nonlinear current fluctuations considered in the work [15], except for two points. (i) Because of the high frequency of light $\omega\tau \gg 1$, the impurity corrections to the single light vertex are neglected. However, just as in [15], the ladder of impurity lines embracing both light vertices are taken into

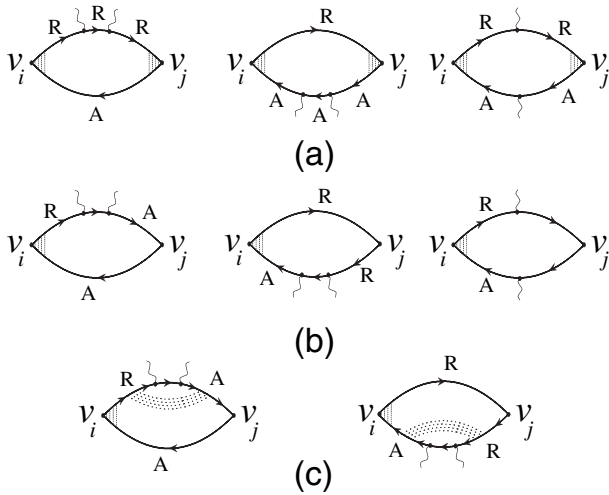


FIG. 1. The diagrams for the changes of the conductivity tensor due to the illumination. The dotted areas denote the impurity-ladder insertions. Note that any of the light vertices of diagrams (b) and (c) can be anomalous.

account because the total frequency of the vertices equals zero. (ii) The impurity ladders relevant to the antisymmetric part of Q_{ij} do not have poles at a real frequency due to the finite spin relaxation time. For this reason, the expansion of σ_H in powers of $E_{\omega}^{(l)}$ does not diverge because of the absence of energy relaxation in the model under consideration. It should also be noted that the symmetric at the $i \rightarrow \leftarrow j$ part of Q_{ij} does not contain the SO coupling within the δ -linear approximation. Therefore, all results of the work [15] are valid for the Q_{ij}^{sim} .

The remarkable result of the developed theory is a property of the impurity-renormalized velocity vertex shown in Fig. 2. The bar velocity operator $\mathbf{v}(\mathbf{p})$, besides the usual scalar part, also has a spin component. A straightforward calculation reveals that at a small difference between frequencies of electron lines entering and leaving the vertex, ($\omega_0 \ll \tau^{-1}\eta^2$), it has the form

$$\mathbf{v}(\mathbf{p}, \omega_0) \cong \frac{\mathbf{p}}{m} - \alpha(\mathbf{c} \times \sigma) \frac{2i\omega_0\tau}{\eta^2}, \quad (6)$$

and hence loses its spin component in the static limit $\omega_0 \rightarrow 0$. It is important that this zero-frequency property is not a result of assumed isotropy of impurity scattering. This can also be proved at s - p approximation for the scattering amplitude and apparently is always true.

The tensor $Q_{ij}(\omega_0)$ of any normal conductor has to be a linear function of ω_0 at $\omega_0 \rightarrow 0$ [13]. Every diagram of Fig. 1(a) obeys this law because it includes the function $F(\epsilon, \omega_0)$ at the driving vertex and $F(\epsilon, \omega_0) \sim \omega_0$ as $\omega_0 \rightarrow 0$; therefore one may set ω_0 equal to zero in the remaining parts of the diagram. Since both the response and driving vertices of the diagram must be renormalized by impurities, they lose their spin parts at $\omega_0 = 0$ because of (6). Thus the ω_0 -linear part of every first class diagram is symmetric under the permutation $i \rightarrow \leftarrow j$ and hence cannot contribute to the Hall conductivity. To show that the total contribution of the second type of diagrams to the antisymmetric part of Q_{ij} disappears at $\omega_0 \rightarrow 0$, one should set ω_0 equal to zero and apply the Ward-like identity

$$\partial G^{R(A)}(\epsilon, \mathbf{p}) / \partial p_j = G^{R(A)}(\epsilon, \mathbf{p}) v_j(\mathbf{p}) G^{R(A)}(\epsilon, \mathbf{p}), \quad (7)$$

that follows from the operator representation of the Green function $G_{\alpha\beta}^{R(A)}(\epsilon, \mathbf{p}) = [\epsilon - H_0(\mathbf{p}) \pm \frac{i}{2\tau}]_{\alpha\beta}^{-1}$ and the relation $\mathbf{v}(\mathbf{p}) = \partial H_0(\mathbf{p}) / \partial \mathbf{p}$, to the driving vertex of these

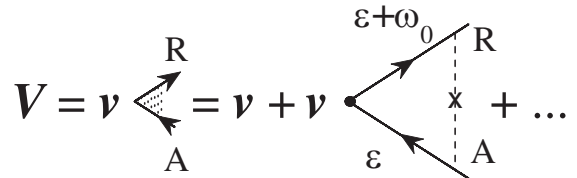


FIG. 2. The diagrams for the impurity-dressed velocity vertex.

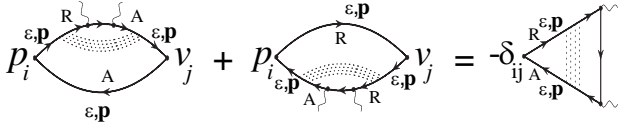


FIG. 3. The relation showing the cancellation of the anti-symmetric parts of the diagrams of Fig. 1(c) at $\omega_0 \rightarrow 0$.

diagrams followed by integration by parts. In this way, one can prove the relation shown in Fig. 3, for diagrams of Fig. 1(c). In the same way, one can obtain an analogous equation for the diagrams of Fig. 1(b) that shows that these diagrams also lose their antisymmetric parts in the static limit. The equation $\lim_{\omega_0 \rightarrow 0} Q_{ij}^{\text{anti}}(\omega_0) = 0$ allows one to write $Q_{ij}^{\text{anti}}(\omega_0) = i\omega_0 \sigma_{ij}^{\text{anti}}$ and consider $\sigma_{ij}^{\text{anti}}$ as the anti-symmetric part of the conductivity tensor. Now the transverse part of the current $Q_{ij}^{\text{anti}} A_j^{(d)}$ takes the usual form $\sigma_{ij}^{\text{anti}} E_j^{(d)}$. For a given second-type diagram, ω_0 -linear terms can be derived either from the impurity-renormalized response vertex $\mathbf{V}(\mathbf{p}, \omega_0)$ or from other parts of the diagram. The total contribution to the transverse current of the ω_0 -linear terms derived from $\mathbf{V}(\mathbf{p}, \omega_0)$ is equal to

$$-(\mathbf{c} \times \mathbf{E}^{(d)}) i(\mathbf{c} \cdot \mathbf{E}_\omega^{(l)} \times \mathbf{E}_\omega^{(l)*}) \frac{3e^4 \tau^2 \eta \delta}{2\pi p_F^2 (\omega\tau)^5}, \quad (8)$$

while the total contribution of the other ω_0 -linear terms equals

$$(\mathbf{c} \times \mathbf{E}^{(d)}) i(\mathbf{c} \cdot \mathbf{E}_\omega^{(l)} \times \mathbf{E}_\omega^{(l)*}) \frac{2e^4 \tau^2 \eta^3 \delta}{\pi p_F^2 (\omega\tau)}. \quad (9)$$

So we come to Eq. (3) [16]. The fact that $\sigma_H \sim \delta$ means that the pseudo-Hall effect takes place just due to the difference between the energy branches $E_\pm(p)$. The same is true for MEE [9], IFE [10], and apparently for any macroscopic property of a conductor induced by the broken mirror symmetry. Thus the asymmetry between electrons of opposite helicities is the main point of the kinetics of mirror-odd conductors.

At small α and not very high frequency of the light, the second term in Eq. (3) dominates; e.g., for the rather dirty $\text{In}_x\text{Ga}_{1-x}\text{As}/\text{In}_y\text{Al}_{1-y}\text{As}$ heterostructure with $\hbar/\tau \approx 10$ meV, $\alpha = 1.4 \times 10^{-10}$ eV cm [2], $m^* = 0.046m_0$,

$n = 6 \times 10^{11}$ cm $^{-2}$, and for the far-infrared (FIR) ($\lambda = 10^{-2}$ cm) pulse laser of power $P = 10^2$ W focused on the structure of dimension 1 mm 2 , one has $2\alpha p_F \approx 0.056$ eV, $\omega\tau \approx 1$, and $\sigma_H/\sigma_D \approx 10^{-6}$. However, for the metal surface bands, where much greater values of $2\alpha p_F$ were found (0.1 eV in Au [3] and up to 0.5 eV in Mo and W [4]), and for the infrared light ($\lambda = 10^{-3}$ cm) the second term in (3) may appear to dominate.

Thus we have shown that the phenomenon similar to the Hall effect can be induced in mirror-odd conductors by the circular light illumination. The effect means that one can control the direction of current with the aid of light. The effect also provides the possibility for measuring the value of α in dirty metals where other methods [2] are inoperative.

This work was supported in part by the Program Spintronics RAS and by Grant No. 04-02-17394 from RFBR.

-
- [1] C.P. Pole, *Handbook of Superconductivity* (Academic, New York, 1999).
 - [2] B. Das *et al.*, Phys. Rev. B **41**, 8278 (1990).
 - [3] S. LaShell *et al.*, Phys. Rev. Lett. **77**, 3419 (1996).
 - [4] E. Rotenberg *et al.*, Phys. Rev. Lett. **82**, 4066 (1999).
 - [5] *Semiconductor Spintronics and Quantum Computation*, edited by D.D. Awschalom, D. Loss, and N. Samarth (Springer, Berlin, 2002).
 - [6] E.I. Rashba, Fiz. Tverd. Tela (Leningrad) **1**, 407 (1959) [Sov. Phys. Solid State **1**, 366 (1959)].
 - [7] See, for example, Y. Kato *et al.*, Nature (London) **427**, 50 (2004), and quoted literature.
 - [8] M.I. Dyakonov and V.I. Perel', Fiz. Tverd. Tela (Leningrad) **13**, 3581 (1971) [Sov. Phys. Solid State **13**, 3023 (1972)].
 - [9] V.M. Edelstein, Solid State Commun. **73**, 233 (1990).
 - [10] V.M. Edelstein, Phys. Rev. Lett. **80**, 5766 (1998).
 - [11] J.M. Luttinger, Phys. Rev. **112**, 739 (1958).
 - [12] S.D. Ganichev *et al.*, Phys. Rev. Lett. **86**, 4358 (2001).
 - [13] A.A. Abrikosov, L.P. Gor'kov, and I.E. Dzyaloshinskii, *Methods of Quantum Field Theory in Statistical Physics* (Prentice Hall, Englewood Cliffs, NJ, 1963).
 - [14] L.P. Gor'kov and G.M. Eliashberg, Zh. Eksp. Teor. Fiz. **54**, 612 (1968) [Sov. Phys. JETP **27**, 328 (1968)].
 - [15] A.-M. Tremblay *et al.*, Phys. Rev. A **19**, 1721 (1979).
 - [16] Details of the calculation will be given elsewhere.